Soy protein isolates prevent loss of bone quantity associated with obesity in rats through regulation of insulin signaling in osteoblasts

Jin-Ran Chen,[*,†,1,2] Jian Zhang,[*,†,1] Oxana P. Lazarenko,[*,‡] Jay J. Cao,[‖] Michael L. Blackburn,[*,‡] Thomas M. Badger,[*,†,‡] and Martin J. J. Ronis[*,†,§]

[*]Arkansas Children's Nutrition Center, Little Rock, Arkansas, USA; [†]Department of Pediatrics, [‡]Department of Physiology and Biophysics, and [§]Department of Pharmacology and Toxicology, University of Arkansas for Medical Sciences, Little Rock, Arkansas, USA; and [‖]Grand Forks Human Nutrition Research Center, Grand Forks, North Dakota, USA

ABSTRACT **In both rodents and humans, excessive consumption of a typical Western diet high in saturated fats and cholesterol is known to result in disruption of energy metabolism and development of obesity and insulin resistance. However, how these high-fat, energy-dense diets affect bone development, morphology, and modeling is poorly understood. Here we show that male weanling rats fed a high-fat (HF) diet containing 45% fat and 0.5% cholesterol made with casein (HF-Cas) for 6 wk displayed a significant increase in bone marrow adiposity and insulin resistance. Substitution of casein with soy protein isolate (SPI) in the HF diet (HF-SPI) prevented these effects. Maintenance of bone quantity in the SPI-fed rats was associated with increased undercarboxylated osteocalcin secretion and altered JNK/IRS1/Akt insulin signaling in osteoblasts. The HF-Cas group had significantly greater serum nonesterified free fatty acid (NEFA) concentrations than controls, whereas the HF-SPI prevented this increase. *In vitro* treatment of osteoblasts or mesenchymal stromal ST2 cells with NEFAs significantly decreased insulin signaling. An isoflavone mixture similar to that found in serum of HF-SPI rats significantly increased *in vitro* osteoblast proliferation and blocked significantly reduced NEFA-induced insulin resistance. Finally, insulin/IGF1 was able to increase both osteoblast activity and differentiation in a set of *in vitro* studies. These results suggest that high-fat feeding may disrupt bone development and modeling; high concentrations of NEFAs and insulin resistance occurring with high fat intake are mediators of reduced osteoblast activity and differentiation; diets high in soy protein may help prevent high dietary fat-induced bone impairments; and the molecular mechanisms underlying the SPI-protective effects involve isoflavone-induced normalization of insulin signaling in bone.—Chen, J.-R., Zhang, J., Lazarenko, O. P., Cao, J. J., Blackburn, M. L., Badger, T. M., Ronis, M. J. J. Soy protein isolates prevent loss of bone quantity associated with obesity in rats through regulation of insulin signaling in osteoblasts. *FASEB J.* 27, 3514–3523 (2013). www.fasebj.org**

Key Words: high-fat diet · free fatty acid · isoflavone · osteocalcin

Postnatal development of obesity is associated with excessive consumption of a Western diet (defined as having high levels of saturated fat and cholesterol). Feeding a high-fat (HF) diet to rodents has been reported to result in systemic insulin resistance and metabolic syndrome (1). Development, maturation, and modeling of the skeletal system in the pediatric population are affected by nutritional status, dietary factors, body composition, and the effects of weight bearing (2). Increased bone marrow adiposity and systemic insulin resistance are common features of impaired bone quality/quantity in patients with a variety of conditions, such as obesity, chronic alcohol abuse, diabetes mellitus, and aging (3–6). Therefore, it is possible that insulin signaling in bone is critical for maintaining bone marrow adiposity and bone mass at a well-balanced level.

A variety of hormones and metabolites are elevated in plasma of obese animals and humans, including insulin, glucose, leptin, insulin-like growth factor 1 (IGF1), and nonesterified free fatty acid (NEFA) concentrations (7–11). Recent evidence in mice has shown that the secretion of osteocalcin, particularly undercarboxylated osteocalcin, an osteoblast-derived active form of the hormone, regulates insulin secretion, insulin sensitivity, and energy expenditure in bone (12). Insulin receptor signaling in osteoblasts has been suggested as

Abbreviations: ALP, alkaline phosphatase; Cas, casein; H&E, hematoxylin and eosin; HF, high fat; IGF1, insulin-like growth factor 1; IRS1, insulin receptor substrate1; LF, low fat; NEFA, nonesterified free fatty acid; OGTT, oral glucose tolerance test; PND, postnatal day; RT-PCR, reverse transcription-polymerase chain reaction; SPI, soy protein isolate

[1] These authors contributed equally to this work.

[2] Correspondence: Arkansas Children's Nutrition Center, 15 Children's Way, Slot 512-20B, Little Rock, AR 72202, USA. E-mail: chenjinran@uams.edu

doi: 10.1096/fj.12-226464

This article includes supplemental data. Please visit *http://www.fasebj.org* to obtain this information.

0892-6638/13/0027-3514 © FASEB

a positive regulator of postnatal bone acquisition (13). Particularly, recent clinical data have shown that being overweight with insulin resistance and visceral adiposity adversely influence adolescence bone mass (14).

Effective approaches to manage obesity are extremely limited. Medication, weight loss programs, and dietary interventions have been the most widely used. However, presently there are only 2 medications approved in the United States for long-term use, and they are associated with a variety of side effects (15). Weight-loss programs have been successful; however, they are often accompanied by significant bone loss, especially without appropriate nutritional supplementation (16, 17). Furthermore, obese children present a special problem, because appropriate interventions would need to improve body composition while simultaneously maintaining normal growth. Dietary intervention may be a more appropriate choice. In this regard, a soy protein isolate (SPI) diet has been investigated as a candidate for the prevention of metabolic syndrome in early development (18). Soy foods have been reported to have a variety of health benefits including improved insulin sensitivity, weight management, and improved body composition (19). Prevention of bone loss in both adult humans and animal models of osteoporosis has also been reported for soy foods (20–22). Activation of AMP-kinase in adipose tissue and skeletal muscle has been implicated in the improvement in lipid and glucose signaling after soy feeding in mice (23). The effects of a soy diet on bone have been attributed to potential estrogenic actions related to its high content of phytoestrogens such as genistein and daidzein, which are isoflavones structurally similar to 17β-estradiol (24–26). Dietary factors other than isoflavone components, including uncharacterized peptides appearing in serum after feeding soy diets, may have effects on bone and other organ systems. We have recently demonstrated positive actions of soy diet on systemic insulin resistance (18).

The current study was designed to explore the potential link between NEFA, insulin sensitivity, and osteoblastic cell differentiation and activity in the young HF fed rat as a model of childhood obesity. Our data suggest that NEFA, bone insulin resistance, and reduced osteoblastic cell differentiation and activity appear to be central mediators of HF-induced impairment of bone development and modeling. We further found that SPI-containing diets blocked the impairment of bone formation and modeling during early development, and this occurs with reduced bone adiposity and improved bone insulin sensitivity.

MATERIALS AND METHODS

Animals and diets

Male Sprague-Dawley rats were purchased from Harlan Industries (Indianapolis, IN, USA), arrived on postnatal day (PND) 20, and on PDN24 were randomly assigned to one of 4 groups (n=10). Rats were fed one of 4 diets: a standard low-fat (LF; 5%) AIN-93G diet formulated with casein (Cas) as the sole protein (LF-Cas); an LF diet made with the AIN-93G diet formula, except that Cas was replaced with SPI (LF-SPI); an HF/high-cholesterol diet containing 18.8 MJ/g energy, 195 g/kg Cas protein, 483 g/kg carbohydrate, 210 g/kg anhydrous milk fat, 5 g/kg cholesterol, and 50 g/kg cellulose fiber (HF-Cas); and the same HF diet as the preceding, except thatCas was replaced by SPI (HF-SPI) plus supplemental amino acids. Thus, there were 2 LF diets, one with Cas (LF-Cas) and one with SPI (LF-SPI), and 2 HF diets, one with Cas (HF-Cas) and one with SPI (HF-SPI). Rats were fed their respective diets from PND24 to PND68. The HF-SPI group had *ad libitum* access to food and water, but the other 3 groups were pair fed to the HF-SPI based on total calories. Since pair-fed rats consumed all their food, consumption was tightly controlled among the 4 groups. Rats were housed in an Association for Assessment and Accreditation of Laboratory Animal Care-approved animal facility at the Arkansas Children's Hospital Research Institute with constant humidity and lights on from 06:00 to 18:00 at 22°C. Physical activity among groups of animals was expected to be similar. All animal procedures were approved by the Institutional Animal Care and Use Committee at University of Arkansas for Medical Sciences. Rat body weights were monitored 2×/wk. At 7 d prior to killing, rats were given a standard oral glucose tolerance test (OGTT), and tail blood was taken as described previously (18). At the completion of the experiment, rats were anesthetized by injection with 100 mg nembutal/kg body weight (Avant Laboratories, Avant, OK, USA), followed by decapitation, and legs and serum were collected. Gonadal and abdominal fat tissues were also taken, and their weights were recorded. Serum insulin concentrations were measured using an ELISA (EZRMI-13K) for rat serum (Linco Research, St. Charles, MO, USA). Serum glucose was measured using the glucose oxidase method (IR070; Synermed, Westfield, IN, USA).

Bone analyses

Micro-computed tomography (CT) measurements of trabecular of the tibial bone were evaluated using a Scanco microCT scanner (μCT-40; Scanco Medical AG, Bassersdorf, Switzerland) at 6 μm isotropic voxel size with an X-ray source power of 55 kV and 145 μA and integration time of 300 ms. The grayscale images were processed by using a low-pass gaussian filter (σ=0.8, support=1) to remove noise, and a fixed threshold of 220 was used to extract the mineralized bone from the soft tissue and marrow phase. Cancellous bone was separated from the cortical regions by semiautomatically drawn contours. A total of 120 slices starting from ~1 mm distal to growth plate, constituting 0.70 mm length, was evaluated for trabecular bone structure by using software provided by Scanco, as described in detail previously (27).

Bone hematoxylin and eosin (H&E) staining on decalcified tibia sections was carried out using the standard protocol from a VectaStain ABC kit (Vector Laboratory, Burlingame, CA, USA).

Serum bone turnover markers and NEFAs

The serum bone formation marker alkaline phophatase (ALP) and the serum bone resorption marker procollagen cross-links RatLaps were measured by Rat-MID ALP ELISA and RatLaps ELISA, respectively, from Nordic Biosciences Diagnostic (Herlev, Denmark). Serum undercarboxylated osteocalcin and total osteocalcin (including in culture medium) levels were measured by an ELISA-based kit from Takara Bio (Otsu, Japan). An ELISA test for a carboxy-terminal peptide fragment of type 1 collagen levels was performed using enzyme immunoassay kits from TSZ ELISA (TSZ Scientific, Framingham, MA, USA). Total NEFAs (Wako Diagnostics; Wako Chemicals, Richmond, VA, USA) were measured using standard ELISA method according to proce-

dures provided by the manufacturer. NEFA composition in serum was characterized and quantified using a Shimadzu QP-2010 GC-MS (Shimadzu Corp., Kyoto, Japan) after TLC separation.

Cell culture

Bone marrow stromal cell line ST2 or osteoblastic cell line OB6 was cultured in α-MEM supplemented with 10% FBS (Hyclone, Logan, UT, USA), penicillin (100 U/ml), streptomycin (100 μg/ml), and glutamine (4 mM). For different assay purposes (mRNA, proteins), different sizes of cell culture plates were used, and cells were treated in the presence or absence of NEFAs, isoflavone, insulin, and IGF1 for different durations (see Results). Free acids were dissolved in 95% ethanol at 60°C and then mixed with prewarmed BSA (10%) to yield a stock concentration of 8 mM. Working concentrations of NEFAs and isoflavone were adjusted to ratios similar to their appearance in serum from HF-Cas and SPI diet rats respectively. Individual isoflavones were purchased from Plantec, Reading, UK, and NEFAs were purchased from Sigma-Aldrich (St. Louis, MO, USA).

Western blotting and coimmunoprecipitation

Right tibial bone tissue and *in vitro* cellular proteins were extracted for Western immunoblot analysis using cell lysis buffer as described previously (10). Briefly, after cleaning of surrounding connective tissues and aspiration of bone marrow cells, tibia was smashed to small pieces using surgical pliers. After adding ~400 ml of cell lysis buffer, bone tissues were homogenized using a tissue homogenizer. Western blot and coimmunoprecipitation analyses were performed using standard protocols. The following primary antibodies were used: p-IRS1(Ser307); rabbit, polyclonal (catalog no. 07-247; Millipore, Billerica, MA, USA); p-IRS1(Tyr612), rabbit, polyclonal (ab66153; Abcam, Cambridge, MA, USA); T-IRS1, rabbit, polyclonal (2382; Cell Signaling; Danvers, MA, USA); p-Akt, rabbit, polyclonal (sc-135650; Santa Cruz Biotechnology, Santa Cruz, CA, USA); T-Akt, rabbit, polyclonal (9272; Cell Signaling); β-actin, mouse, monoclonal (a1978; Sigma-Aldrich); p-JNK, mouse, monoclonal (J4750; Sigma-Aldrich); and T-JNK, mouse monoclonal (SAB4200176; Sigma-Aldrich). Secondary antibodies were purchased from Santa Cruz Biotechnology (goat anti-rabbit IgG, sc-2004; goat anti-mouse IgG, sc-2005). Blots were developed using chemiluminescence (Pierce Biotechnology, Rockford, IL, USA) according to the manufacturer's recommendations.

RNA isolation, real-time reverse transcription-polymerase chain reaction (RT-PCR)

RNA from bone tissues or cultured cells was isolated and extracted using TRI Reagent (MRC Inc., Cincinnati, OH, USA) according to the manufacturer's recommendation, followed by DNase digestion and column cleanup using Qiagen minicolumns (Qiagen, Valencia, CA, USA; ref. 28). Reverse transcription was carried out using an iScript cDNA synthesis kit from Bio-Rad (Hercules, CA, USA). All primers for real-time PCR analysis used in this report were designed using Primer Express 2.0.0 software (Applied Biosystems, Foster City, CA, USA) and are listed in Supplemental Table S1.

Statistical analyses

Numerical variables are expressed as means ± SEM. Comparisons between groups were performed with the nonparametric Kruskall-Wallis test, followed with 2-by-2 comparisons performed with a Mann-Whitney *U* test adjusted for multiple comparisons. For paired measures, the nonparametric Wilcoxon matched-pairs signed-ranks test was used. The critical *P* value for statistical significance was $P = 0.05$.

RESULTS

SPI prevents HF-induced obesity, bone marrow adiposity, and insulin resistance in bone

Rats were fed LF or HF diets made with either Cas or SPI. Rats were pair-fed the HF-SPI diet. HF-Cas-fed rats were heavier than LF-Cas-fed rats: 465.0 ± 12.1 *vs.* 395.5 ± 19.7 g, respectively ($P=0.026$). LF-SPI-fed rats had the lowest body weight ($P<0.05$), and HF-SPI-fed rats had body weights similar to the LF-Cas group (**Fig. 1*A***), suggesting that SPI-containing diets protected against HF-induced weight gains. When regional fat pads were expressed as percentage of body weight, the HF-Cas-fed rats had larger abdominal fat pads (1.61±0.21%) and gonadal fat pads (1.39±0.11%) than LF controls (0.85±0.08 and 0.81±0.0%, respectively; $P<0.05$). The LF-SPI diet group had smaller gonadal fat pads ($P<0.05$), but similar abdominal fat pads compared with LF-Cas-fed rats (Fig. 1*B*). Thus, SPI was able to prevent HF-induced increases in rat body fat.

We performed an OGTT, and tail blood insulin concentration measurement at PND61. In HF-Cas-fed animals, greater serum glucose and insulin concentrations were found at 60, 90, and 150 min after glucose challenge compared with the other groups ($P<0.05$; Fig. 1*C*). Insulin sensitivity was the greatest in the LF-SPI group and similar between the LF-Cas and HF-SPI groups (Fig. 1*D*). This was accompanied by prevention of hyperglycemia in the HF-SPI group compared with the HF-Cas group (Fig. 1*C*).

To determine whether SPI could block or prevent bone marrow adiposity, analyses of tibia bone/bone marrow histology were conducted. H&E staining revealed the HF-Cas-fed rats had excessive fat deposition in the bone marrow, while bone marrow adiposity did not differ significantly between LF-Cas, LF-SPI, and HF-SPI groups (**Fig. 2*A***). We examined insulin signaling in bone tissue and found that phosphorylation at the inhibitory site Ser307 on insulin receptor substrate 1 (IRS1) was substantially increased while phosphorylation of Tyr612 was decreased on IRS1 in the bone of HF-Cas-fed rats (Fig. 2*B*) despite total IRS1 appearing to be lower in the HF-Cas group. No effects were found in the other groups, suggesting that SPI blocked HF-induced phosphorylation of IRS1 in bone. In accordance with these data, Akt phosphorylation was markedly down-regulated in bone from the HF-Cas group compared to the LF-Cas group (Fig. 2*B*). The LF-SPI diet group increased Akt (Thr308) phosphorylation in bone compared with LF-Cas (Fig. 2*B*). Consistent with previous data in mouse liver (29), rats fed HF-Cas also exhibited a substantial elevation of JNK phosphorylation in bone (Fig. 2*B*). There were no significant differences in JNK phosphorylation status among the other groups (Fig. 2*B*). Phosphorylated IRS1 (Ser307

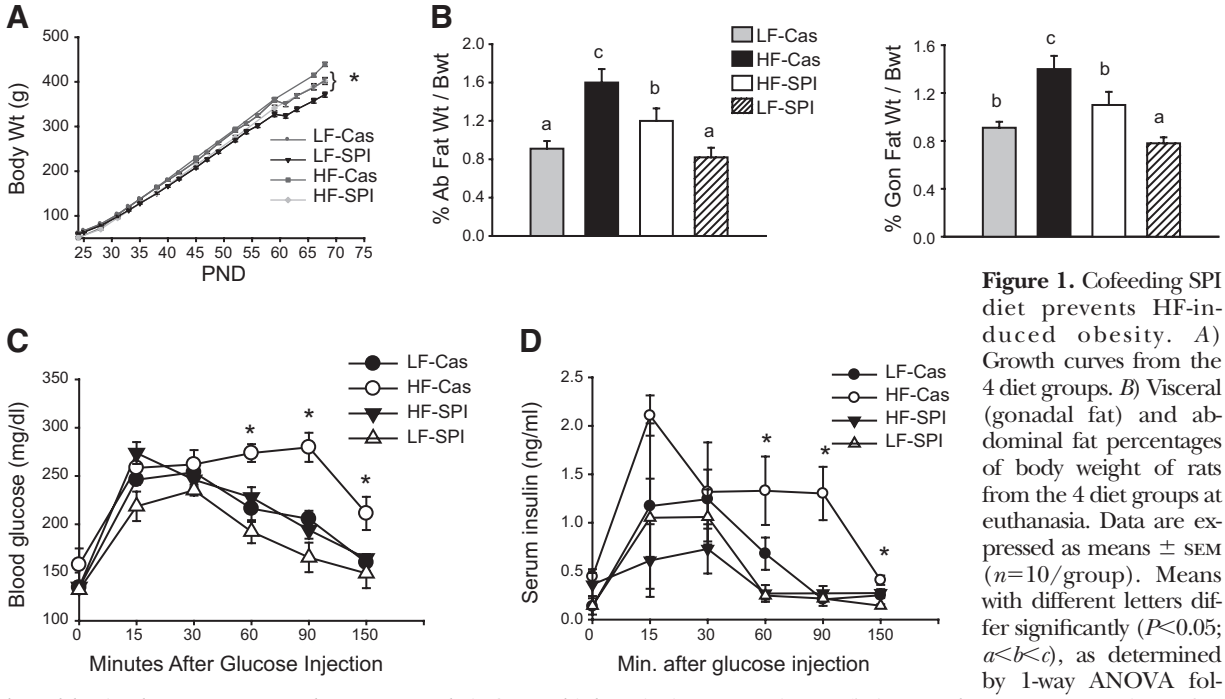

Figure 1. Cofeeding SPI diet prevents HF-induced obesity. *A*) Growth curves from the 4 diet groups. *B*) Visceral (gonadal fat) and abdominal fat percentages of body weight of rats from the 4 diet groups at euthanasia. Data are expressed as means ± SEM (n=10/group). Means with different letters differ significantly (P<0.05; a<b<c), as determined by 1-way ANOVA followed by Student-Newman-Keuls *post hoc* analysis for multiple pairwise comparisons. *C*) Serum glucose concentrations after OGTT in PND61 rats fed 4 different diets from PND24. Data are means ± SEM, n = 10 rats. Animals were denied access to food overnight, and tail blood was sampled over a 150-min period following a 2.5 g/kg oral glucose challenge. *D*) Serum insulin concentration after an OGTT in PND61 rats fed 4 different diets. *$P < 0.05$ *vs.* LF-Cas and HF-Cas groups.

and phosphorylated JNK were coimmunoprecipitated with JNK when bone proteins from HF-Cas-fed rats were subjected to a coimmunoprecipitation experiment (Fig. 2*C*). SPI diet prevented this HF-induced increase of p-JNK and p-IRS1 association in bone (Fig. 2*C*).

SPI prevents HF-induced impairment of bone quality

MicroCT analysis of tibial bones revealed their phenotypes represented in images presented in **Fig. 3*A***. Specifically, bone volume, trabecular number, and trabecular thickness were all decreased in HF-Cas-fed rats compared to LF-Cas-fed animals (Fig. 3*B*). These parameters were highest in the LF-SPI group (Fig. 3*B*). However, trabecular spacing was greater in HF-Cas-fed rats compared with the other groups. Impaired bone acquisition in HF-Cas-fed rats was consistent with our previous observations in which we utilized a rat total enteral nutrition model of HF feeding, while keeping the body weights equal between groups, to demonstrate that low bone quality was associated with development of obesity (10). Serum bone turnover marker measurements revealed that osteocalcin levels were lower in HF-Cas-fed rats compared to the LF-Cas diet group (**Table 1**). Undercarboxylated osteocalcin, an endocrine active form of osteocalcin secreted only by osteoblasts, was found to be the highest in the LF-SPI group, and decreased in the HF-Cas-fed rats compared to LF-Cas group (Table 1). There were no differences between HF-SPI and LF-Cas groups, and this is reflected in the bone mass data presented in Fig. 3. Serum NEFA concentrations in HF-Cas-fed rats were almost 3 times higher than those in LF-Cas-fed rats (Table 1), while these levels did not differ among the other groups compared to LF-Cas. Serum NEFA composition of HF-Cas-fed rats was also characterized and quantified using a Shimadzu QP-2010 GC-MS after TLC separation. We found that there were 5 major fatty acids with ratios similar to results previously reported in our laboratory (10), with palmitate (~200 μM) having the highest concentration of fatty acids in serum of HF-Cas-diet rats (data not shown). Quantitative real-time PCR analysis of osteocalcin mRNA expression in bone was very similar to its pattern in serum (Fig. 3*C* and Table 1). Gene expression of another osteoblastic cell activity marker, collagen type 1 (Col1), was also lower in HF-Cas-fed rats compared to LF-Cas-fed rats (Fig. 3*C*). There were no differences in Col1 mRNA expression between the LF-SPI groups and HF-SPI controls (Fig. 3*C*).

Role of NEFAs

NEFAs from increased fat stores may be one of the most important factors affecting bone in obesity. SPI consumption results in appearance of many bioactive compounds in blood. To date, isoflavones are the most studied components associated with dietary soy and have been found to have beneficial effects on bone (30). Therefore, we assessed the serum isoflavone levels in rats fed SPI diets using a method previously published in our laboratory (31, 32). Total isoflavone concentrations were in the range of 1 μM, and the major isoflavone was the estrogenic daidzein metabolite equol (32, 33). Next, osteoblastic OB6 cells were treated with NEFAs in the presence or absence of isoflavones. Concentration and ratios of individual

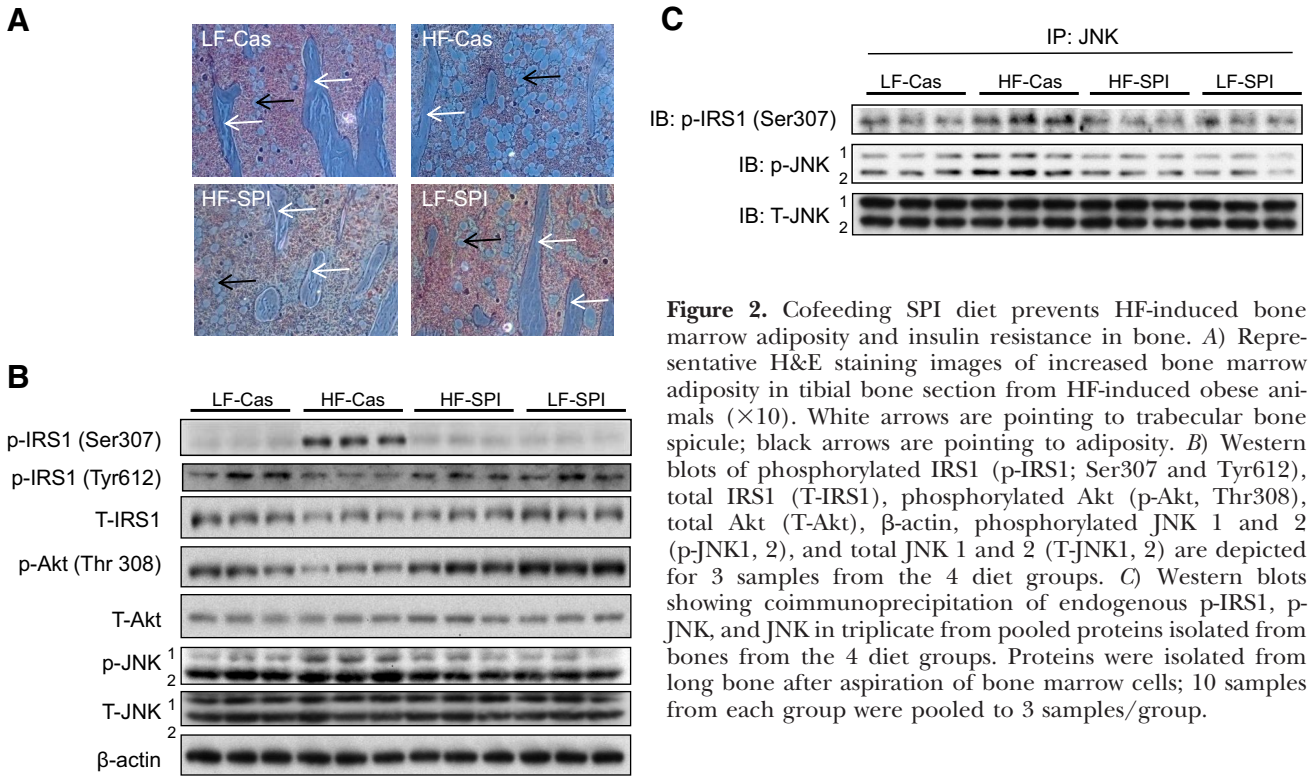

Figure 2. Cofeeding SPI diet prevents HF-induced bone marrow adiposity and insulin resistance in bone. *A*) Representative H&E staining images of increased bone marrow adiposity in tibial bone section from HF-induced obese animals (×10). White arrows are pointing to trabecular bone spicule; black arrows are pointing to adiposity. *B*) Western blots of phosphorylated IRS1 (p-IRS1; Ser307 and Tyr612), total IRS1 (T-IRS1), phosphorylated Akt (p-Akt, Thr308), total Akt (T-Akt), β-actin, phosphorylated JNK 1 and 2 (p-JNK1, 2), and total JNK 1 and 2 (T-JNK1, 2) are depicted for 3 samples from the 4 diet groups. *C*) Western blots showing coimmunoprecipitation of endogenous p-IRS1, p-JNK, and JNK in triplicate from pooled proteins isolated from bones from the 4 diet groups. Proteins were isolated from long bone after aspiration of bone marrow cells; 10 samples from each group were pooled to 3 samples/group.

NEFAs and isoflavones were similar to their appearance in the serum of rats from HF and SPI, respectively. As to NEFAs, 5 major fatty acids, palmitic, stearic, oleic, linoleic, and arachidonic acid, were mixed in the ratio of 5:1:2:3:1 at concentrations appearing in the serum of HF-Cas-fed rats. Similarly, isoflavones is the mixture of glycetein, genistein, daidzein, and equol with concentration of each individual compound similar to their level in animal serum after SPI diet. Treatment of cells with this NEFA mixture for 3 d significantly decreased, whereas isoflavones increased, osteoblast proliferation, reflected by the changes in osteoblast numbers (**Fig. 4*A***). However, isoflavones did not block NEFA-induced down-regulation of osteoblast proliferation (Fig. 4*A*); suggesting that NEFAs and isoflavones have independent effects on osteoblastic cell proliferation. To further obtain mechanistic explanations for our *in vivo* observations, we next studied insulin signaling in osteoblasts after 24 h treatment with NEFAs in the presence or absence of isoflavones. We found that NEFAs not only phosphorylated IRS1 at its inhibitory site Ser307, it also inhibited total IRS1 expression (Fig. 4*B*). More strikingly, NEFAs down-regulated both phosphorylated and total Akt expression (Fig. 4*B*) and substantially phosphorylated JNK (Fig. 4*B*). Isoflavone treatment had opposite effects on osteoblasts, inhibiting IRS1 phosphorylation and up-regulating total IRS1 expression (Fig. 4*B*). Moreover, isoflavones increased Akt phosphorylation and total Akt expression and decreased JNK phosphorylation (Fig. 4*B*). All the above observed effects of NEFAs were completely abrogated by cotreatment of osteoblasts with isoflavones (Fig. 4*B*). In the presence of insulin in the cell culture, the status of p-Akt and p-IRS1 were similar between control and isoflavone treatment (Supplemental Fig. S1). ST2 cells were similarly treated with NEFAs in the presence or absence of isoflavone. NEFAs significantly down-regulated mRNA expression of well-known osteoblastic cell differentiation markers Runx2, osterix, and ALP in ST2 cells (Fig. 4*C*), indicating that NEFAs also suppress osteoblast differentiation, which is consistent with our previously published data (10, 34). Isoflavones did not significantly change Runx2 and osterix mRNA expression, but significantly up-regulated ALP mRNA expression (Fig. 4*C*). However, in the presence of osteoblastic cell differentiation medium (ob medium), isoflavones significantly increased Runx2 and osterix gene expression (Supplemental Fig. S2). Interestingly, isoflavones blocked NEFA-induced down-regulation of osteoblast differentiation markers, with the exception of osterix (Fig. 4*C*). Similar to results shown in osteoblasts, isoflavones completely inhibited the effect of NEFAs on insulin signaling indicated in Western blot results on phosphorylation of IRS1 and Akt in ST2 cells (Fig. 4*D*).

The 4 free fatty acids that mainly compose NEFAs were also individually tested at the concentration that appeared in rat serum to determine their effects on JNK phosphorylation in osteoblasts. Sustained JNK phosphorylation was found in cells treated with palmitic, oleic, and linoleic acid (**Fig. 5*A***). Palmitic acid not only activated JNK, but also increased the phosphorylation of IRS1 (Fig. 5*B*). JNK inhibitor SP600125 abolished the effects of palmitic acid on phosphorylation of both IRS1 and JNK in osteoblasts (Fig. 5*B*). Most important, when osteoblasts were treated with NEFAs, phosphorylated IRS1 and phosphorylated JNK were coimmunoprecipitated with JNK (Fig. 5*C*). Isoflavones prevented this NEFA-induced increased association of p-JNK and p-IRS1 in osteoblasts (Fig. 5*C*). The interaction between phosphorylated IRS1 and JNK associated with NEFA treatment in osteoblasts was similarly

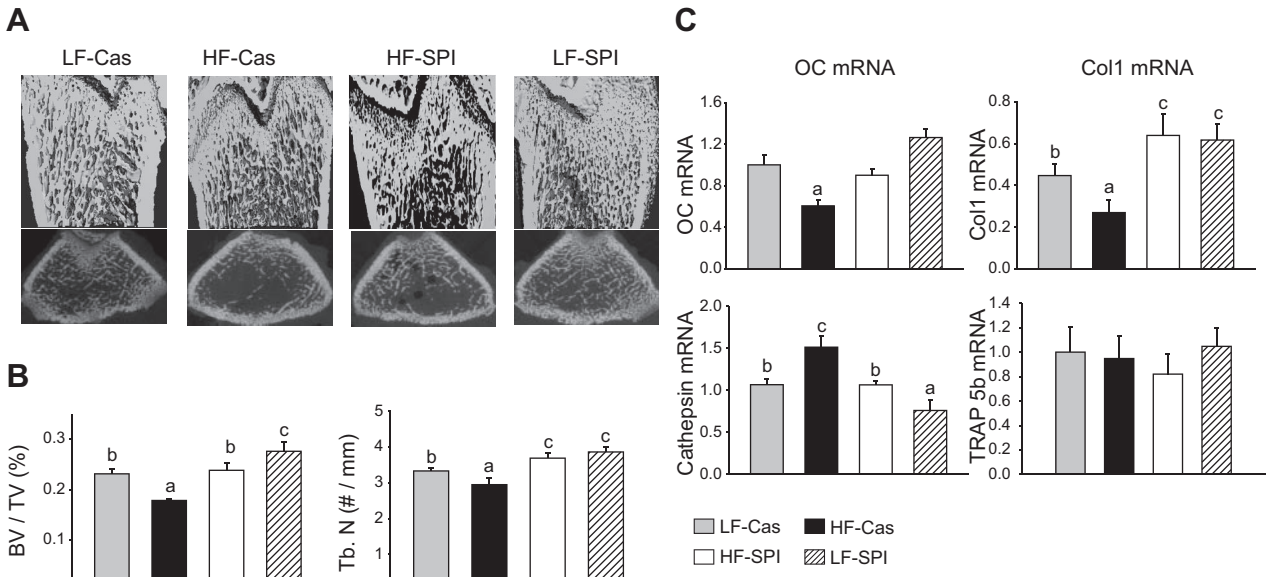

Figure 3. SPI diet prevents HF-induced impairment of rat bone acquisition. *A*, *B*) Quantitative micro-CT analysis of the proximal tibial in rats fed 4 different diets (n=4 rats). *A*) Representative images. *B*) Bone volume/tissue volume (BV/TV; %); trabecular number (Tb. N; no./mm); trabecular thickness (Tb. Th; mm); trabecular spacing (Tb. Sp; mm). *C*) Total RNA isolated from bone and quantitative real-time PCR analyses confirmed the significant down-regulation of osteocalcin gene, as well as Col1 mRNA, from HF-Cas-fed rats compared to those from LF-Cas-fed rats. Cathepsin K is up-regulated in HF-Cas-fed rats. Data are expressed as means ± SEM (n=10/group). Means with different letters differ significantly (P<0.05).

revealed in bone samples (Fig. 1*C*). These data suggest that the effect of HF on insulin signaling in bone *in vivo* and in osteoblasts *in vitro* is, at least in part, due to elevated serum NEFAs. Isoflavones appear to mediate the effects of SPI by attenuating insulin resistance in bone after HF feeding.

Effects of insulin in osteoblastic cells

We have demonstrated that HF or NEFA exposure results in insulin resistance. To address whether insulin has an effect in osteoblastic cells, we treated OB6 and ST2 cells with insulin and IGF1. In OB6 cells, insulin and IGF1 were able to significantly stimulate secretion of osteocalcin and C1CP, a *de novo* collagen synthesis marker measured in cell culture medium (**Fig. 6*A, B***). With insulin or IGF1 treatment, OB6 cells clearly showed increased Akt and IRS1 phophorylation (Fig. 6*D*). In ST2 cells, following treatment with insulin or IGF1, mRNA expression of all 3 osteoblast differentiation markers, ALP, osterix, and Runx2, was significantly increased compared with untreated cells (Fig. 6*C*). Similar to the results we found in OB6 cells, phosphorylation of Akt and IRS1 was higher in ST2 cells following insulin or IGF1 treatment compared to those without treatment (Fig. 6*E*). These data suggest that insulin significantly stimulated osteoblast activity and differentiation *in vitro*.

DISCUSSION

The current study suggests that insulin resistance observed in the bone of rats fed a HF diet may be due to

TABLE 1. *Effects of HF and SPI diet on serum bone turnover markers*

Marker	PND68 male, 6 wk diet			
	LF-Cas	HF-Cas	HF-SPI	LF-SPI
Osteocalcin (ng/ml)	541.3 ± 35.1	479.2 ± 59.7*	519.2 ± 28.8	555.3 ± 62.0
Undercarboxylated osteocalcin (ng/ml)	5.08 ± 0.17	3.97 ± 0.31*	5.03 ± 0.39	5.67 ± 0.27
ALP (μU/min)	0.315 ± 0.05	0.367 ± 0.07*	0.366 ± 0.11	0.368 ± 0.12
RatLaps (ng/m)	30.3 ± 3.8	30.2 ± 4.2	30.6 ± 5.0	31.5 ± 9.7
NEFAs (mM)	0.13 ± 0.01	0.35 ± 0.06*	0.17 ± 0.01	0.11 ± 0.02

Serum bone formation markers total osteocalcin, undercarboxylated osteocalcin, and ALP; resorption marker RatLaps; and NEFA levels were measured using standard ELISA methods. *$P < 0.05$ *vs.* LF-Cas; *t* test.

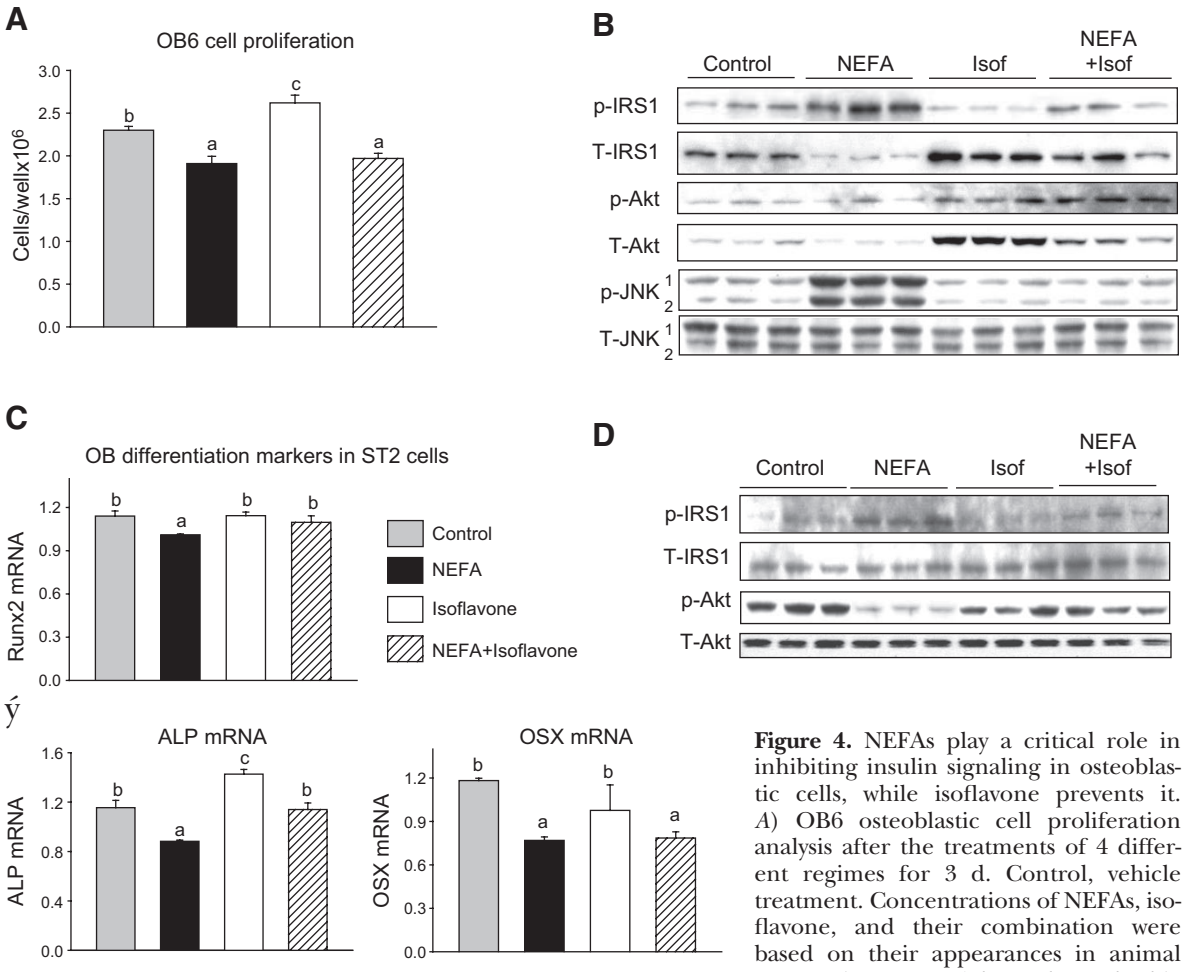

Figure 4. NEFAs play a critical role in inhibiting insulin signaling in osteoblastic cells, while isoflavone prevents it. *A*) OB6 osteoblastic cell proliferation analysis after the treatments of 4 different regimes for 3 d. Control, vehicle treatment. Concentrations of NEFAs, isoflavone, and their combination were based on their appearances in animal serum (see Materials and Methods). *B*) Western blots for phosphorylated and total IRS1, Akt, and JNK in OB6 cells in triplicate after 24 h treatment. *C*) ST2 cells were treated with NEFAs, isoflavone, and their combination for 3 d; cell RNA was isolated, and real-time PCR analyses showed changes in mRNA expression of 3 different osteoblast (OB) differentiation markers, ALP, Runx2, and OSX (osterix). Data are expressed as means ± SEM (triplicate). Means with different letters differ significantly ($P<0.05$). *D*) Western blots for phosphorylated and total IRS1and Akt in ST2 cells in triplicate after 24 h treatment. Isof, isoflavone.

elevated NEFAs. In addition, the impaired bone quantity in rats fed an HF diet may be due to decreased secretion of undercarboxylated osteocalcin, and this is consistent with recently published studies using an osteoblastic cell-specific insulin receptor-knockout animal model in mice (12, 13). SPI incorporated into the HF diet prevents increased bone marrow adiposity, skeletal insulin resistance, and impaired glucose tolerance. This protective effect on bone by SPI appears to be, at least in part, due to the appearance in serum of isoflavones derived from SPI. Although the changes in bone structure may differ between obesity (35) and sex steroid deficiency (26), our results are consistent with the protective effects of isoflavone on bone observed in those previous studies.

It is well known that homeostatic control of blood glucose is determined by 2 major factors: the concentration of insulin in the circulation and insulin sensitivity at target organs. Progression of insulin resistance toward glucose intolerance occurs in obesity due to increased demand for insulin and failure of pancreatic cells to meet this demand (36). While this has been documented for various organs, surprisingly, it has not been established in bone. Bone-forming cells highly express insulin receptor, and a recent rodent study suggested that insulin receptor signaling in osteoblasts is a significant determinant of whole-body glucose homeostasis (37). This is consistent with the results described in the present report. For example, IRS1/Akt/JNK insulin signaling was significantly down-regulated in bone of HF rats. Also, secretion of osteocalcin, especially the undercarboxylated active form, and osteocalcin mRNA expression were significantly lower in bone from HF animals.

Similar to JNK activation in hepatocytes, pancreatic β-cells and other peripheral sites by free fatty acids (38), the mechanisms leading to JNK activation in bone by NEFAs are unknown. However, the consequences may be the same, *i.e.,* inhibition of insulin signaling. Recently, JNK activation was not only shown to be involved in inhibition of insulin signaling by elimination of Akt activation, but also involved in p53-mediated cell senescence pathways (39). It has been reported that p53 is a JNK substrate (40) and pretreatment with

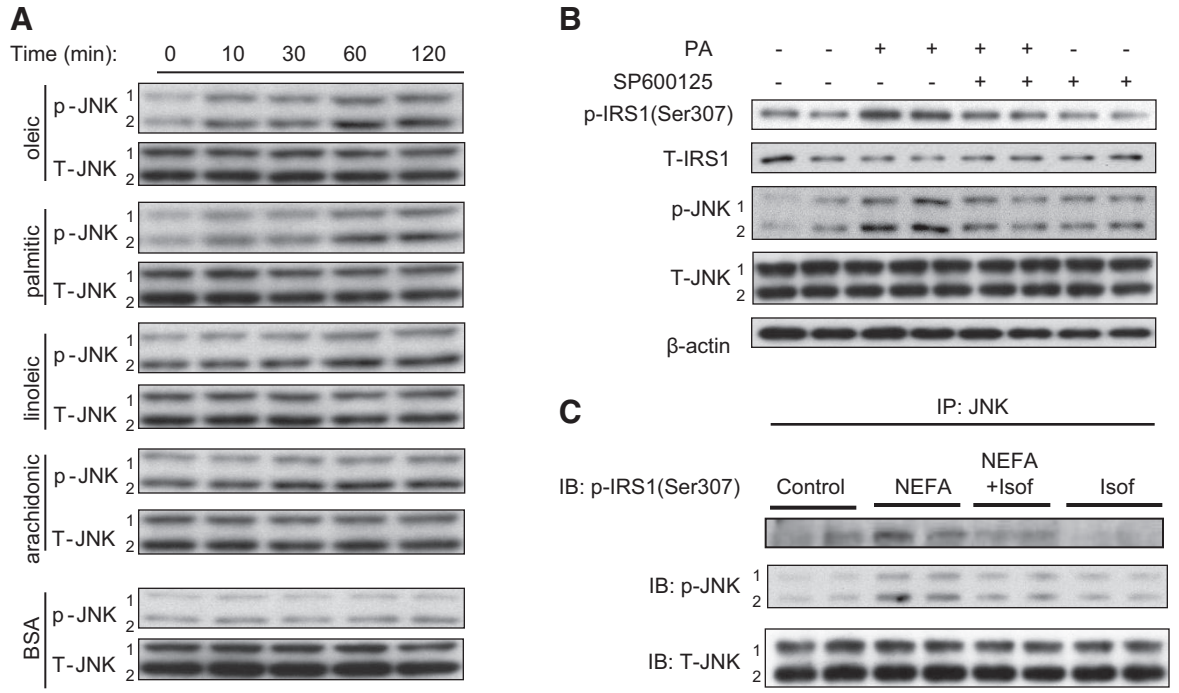

Figure 5. NEFAs activate JNK and IRS1, while isoflavone dissociates them in osteoblasts. *A*) Western blots showing time course of JNK activation (phosphorylation) after OB6 cells were treated with oleic, palmitic, linoleic, arachidonic acid, and BSA as control. *B*) Western blots showing phosphorylation of IRS1 and JNK in OB6 cells after cells were treated with palmitic acid (PA) and JNK inhibitor SP600125 in duplicate for 2 h. *C*) Western blots showing coimmunoprecipitation of endogenous p-IRS1, p-JNK, and T-JNK after OB6 cells were treated with NEFAs, isoflavone, and their combination in duplicate for 2 h.

the specific JNK inhibitor not only decreases senescence, but also induces apoptosis (41). In sharp contrast, JNK deficiency has also been reported to cause p53-dependent senescence in primary murine fibroblasts isolated from embryos (39). Nonetheless, we have shown that increased phosphorylation of JNK along with IRS1 in NEFA-treated osteoblasts resulted in insulin resistance in this particular cell type. Oleic and palmitic acid may be more potent than other NEFAs, and they may be critical *in vivo* in HF-induced obesity

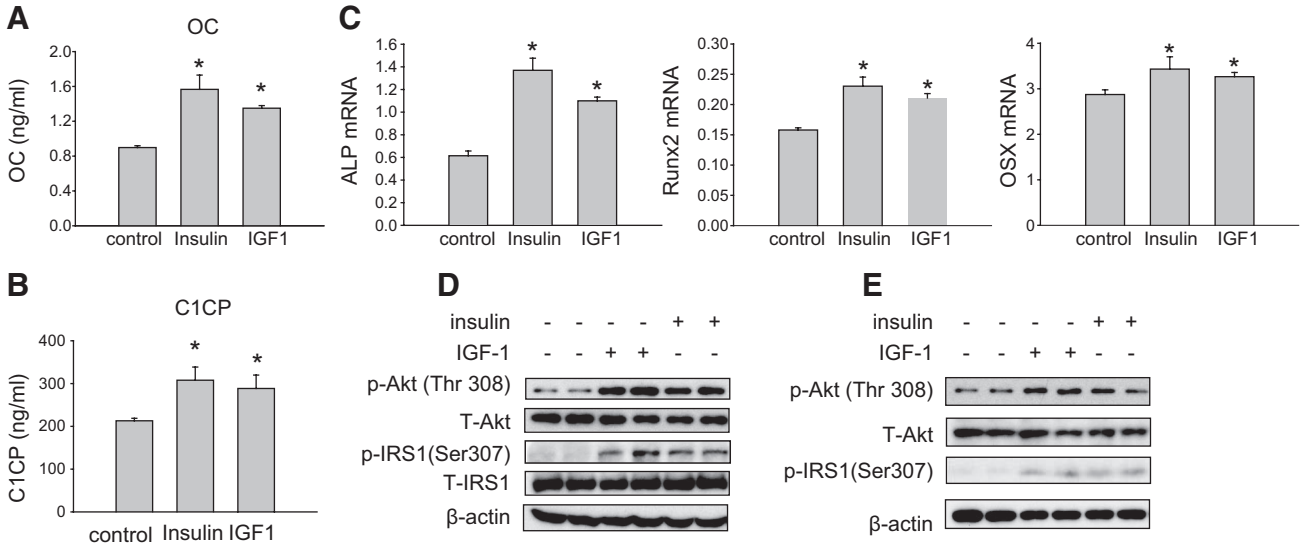

Figure 6. Insulin activates osteoblast and stimulates cell differentiation. *A*, *B*) Secreted osteocalcin (OC; *A*) and cross-linked C-telopeptide of type1 collagen (C1CP; *B*) in culture medium were measured using ELISA after OB6 cells were treated with either insulin or IGF1 (10 nM) for 3 d. *C*) ST2 cells were treated with either insulin or IGF1 (10 nM) for 3 d, and osteoblastic cell differentiation markers ALP, Runx2, and OSX (osterix) mRNA expression were determined using real-time PCR. *D*) OB6 cells were treated with either 10 nM insulin or 10 nM IGF1 for 2 h (duplicated). Western blots for phosphorylated Akt and IRS1, total Akt, IRS1, and β-actin are shown. *E*) ST2 cells were treated with either 10 nM insulin or 10 nM IGF1 for 2 h (duplicated). Western blots for phosphorylated Akt and IRS1, total Akt, and β-actin are shown. $*P < 0.05$ *vs.* control.

leading to JNK activation, IRS Ser/Thr phosphorylation, and down-regulation of insulin receptor signaling in osteoblastic cells. In addition, a previous study has shown that palmitate can exert lipotoxic effects in osteoblasts due to mechanisms relating to fatty acid synthesis and Runx2 binding (42); this may explain the suppressive effects of NEFA on osteoblast differentiation reported in the current study. Insulin induces production of the insulin secretagogue osteocalcin (Fig. 6*A*), which may influence glucose utilization (37). Although we did not provide direct evidence of association between insulin resistance and osteocalcin in osteoblasts in HF rats, insulin resistance was accompanied by decreased undercarboxylated osteocalcin secretion *in vivo*. Osteoblastic cells were further shown to have increased osteocalcin secretion after insulin and IGF1 stimulation. We believe that our present report demonstrates for the first time that insulin resistance is associated with HF feeding in bone and osteoblasts. Interestingly, increased bone marrow adiposity was reported in anorexia nervosa, and this was also associated with insulin resistance (43). Such insulin resistance occurring in osteoblasts may directly alter the function of cells leading to bone deterioration. Using genetically modified animal models, it may be possible to untangle this relationship.

Significant decreases in both gonadal and abdominal fat pad weights in the HF group with coadministration of SPI are consistent with recent studies demonstrating that soy-containing diets or soy diet-derived phytoestrogens, such as genistein, have antilipogenic effects in ovariectomized rodents (44) and effects on osteoblastic cell differentiation (45). Moreover, previous studies have also shown that dietary soy protein reduces cardiac lipid accumulation and ceramide concentration in HF diet-fed rats and ob/ob mice (46). These findings agreed with our recently published data, which revealed that feeding SPI-containing diets blocked HF-induced systemic insulin resistance and maintained lipid homeostasis (18). Our current results were consistent with our previous observation in which both soy infant formula-fed infants and piglets showed lower total body fat but increased bone acquisition rate compared to controls (47). Compared with HF alone, serum NEFA levels in the HF-SPI group were significantly decreased in the present study, reflecting adipose tissue mass as the primary source for NEFA rather than HF diet itself. Although the positive effect of SPI on trabecular bone is consistent with our previous observations, the current data also indicated that bone mass was significantly protected from the effects of HF by SPI. We believe that this may be clinically applicable. In both humans and experimental animals, the most recent studies on dietary intervention for obesity use a caloric restrictive diet, but this diet is linked to a concomitant accelerated bone loss and increased risk of fracture (48, 49). The protective effect of SPI diet on decreased bone acquisition associated with HF feeding has been suggested to be due at least in part to isoflavones. Since these SPI-associated isoflavones are structurally similar to 17-β-estradiol, a majority of the research has focused on their estrogenic effects on bone (45); they may also exert nonestrogenic effects on bone (30, 33). We have recently addressed such differential effects between SPI and estrogen on bone (33). However, to definitively elucidate isoflavones anti-NEFA effect on bone, an *in vivo* isoflavone and NEFA coadministration experiment may be necessary in future studies.

In summary, feeding young prepubertal rats a diet composed of Cas protein and high in saturated fat and cholesterol produced adiposity characterized by increased bone marrow fat stores, bone insulin resistance, and compromised bone quality. High levels of NEFAs acting through undercarboxylated osteocalcin secretion and IRS1/Akt insulin signaling in osteoblasts were shown to impair bone quality *in vitro*. Replacing Cas protein in the HF diet with SPI prevented bone adiposity and bone insulin resistance, and this was associated with lower serum NEFA concentrations and improved bone quality. Isoflavones were shown *in vitro* to prevent NEFA-induced impairment of osteoblast differentiation and insulin signaling pathway and therefore are candidates for the bioactive components within SPI responsible for preventing HF-induced bone impairment in rats. FJ

This work was supported in part by U.S. Department of Agriculture (USDA)/Agricultural Research Service (ARS) grant CRIS 6251-51000-003 to the Arkansas Children's Nutrition Center and CRIS 5450–51000-046-00D to the Grand Forks Human Nutrition Research Center (J.J.C.).

REFERENCES

1. Grund, S. M. (2004) Obesity, metabolic syndrome, and cardiovascular disease. *J. Clin. Endocrinol. Metab.* **89,** 2595–2600
2. Davies, J. H., Evans, B. A., and Gregory, J. W. (2005) Bone mass acquisition in healthy children. *Arch. Dis. Child.* **90,** 373–378
3. Taylor, E. D., Theim, K. R., Mirch, M. C., Ghorbani, S., Tanofsky-Kraff, M., Adler-Wailes, D. C., Brady, S., Reynolds, J. C., Calis, K. A., and Yanovski, J. A. (2006) Orthopedic complications of overweight in children and adolescents. *Pediatrics* **117,** 2167–2174
4. Chen, J. R., Lazarenko, O. P., Shankar, K., Blackburn, M. L., Badger, T. M., and Ronis, M. J. (2010) A role for ethanol-induced oxidative stress in controlling lineage commitment of mesenchymal stromal cells through inhibition of Wnt/beta-catenin signaling. *J. Bone Miner. Res.* **25,** 1117–1127
5. Botolin, S., and McCabe, L. R. (2007) Bone loss and increased bone adiposity in spontaneous and pharmacologically induced diabetic mice. *Endocrinology* **148,** 198–205
6. Shea, M. K., Gundberg, C. M., Meigs, J. B., Dallal, G. E., Saltzman, E., Yoshida, M., Jacques, P. F., and Booth, S. L. (2009) Gamma-carboxylation of osteocalcin and insulin resistance in older men and women. *Am. J. Clin. Nutr.* **90,** 1230–1235
7. Reid, I. R. (2008) Relationships between fat and bone. *Osteoporos. Int.* **19,** 595–606
8. Karsenty, G. (2006) Convergence between bone and energy homeostases: leptin regulation of bone mass. *Cell Metab.* **4,** 341–348
9. He, J., Rosen, C. J., Adams, D. J., and Kream, B. E. (2006) Postnatal growth and bone mass in mice with IGF-I haploinsufficiency. *Bone* **38,** 826–835
10. Chen, J. R., Lazarenko, O. P., Wu, X., Tong, Y., Blackburn, M. L., Shankar, K., Badger, T. M., and Ronis, M. J. (2010) Obesity reduces bone density associated with activation of PPARγ and suppression of Wnt/β-catenin in rapidly growing male rats. *PLoS One* **5,** e13704
11. Takeda, S., Elefteriou, F., Levasseur, R., Liu, X., Zhao, L., Parker, K. L., Armstrong, D., Ducy, P., and Karsenty, G. (2002)

Leptin regulates bone formation via the sympathetic nervous system. *Cell* **111,** 305–317
12. Ferron, M., Wei, J., Yoshizawa, T., Del Fattore, A., DePinho, R. A., Teti, A., Ducy, P., and Karsenty, G. (2010) Insulin signaling in osteoblasts integrates bone remodeling and energy metabolism. *Cell* **142,** 296–308
13. Fulzele, K., Riddle, R. C., DiGirolamo, D. J., Cao, X., Wan, C., Chen, D., Faugere, M. C., Aja, S., Hussain, M. A., Brüning, J. C., and Clemens, T. L. (2010) Insulin receptor signaling in osteoblasts regulates postnatal bone acquisition and body composition. *Cell* **142,** 309–319
14. Pollock, N. K., Bernard, P. J., Gutin, B., Davis, C. L., Zhu, H., and Dong, Y. (2011) Adolescent obesity, bone mass, and cardiometabolic risk factors. *J. Pediatr.* **158,** 727–734
15. Baile, C. A., Yang, J. Y., Rayalam, S., Hartzell, D. L., Lai, C. Y., Andersen, C., and Della-Fera, M. A. (2011) Effect of resveratrol on fat mobilization. *Ann. N. Y. Acad. Sci.* **1215,** 40–47
16. Schwartz, A. V., Johnson, K. C., Kahn, S. E., Shepherd, J. A., Nevitt, M. C., Peters, A. L., Walkup, M. P., Hodges, A., Williams, C. C., Bray, G. A., and Look AHEAD Research Group. (2012) Effect of one year of an intentional weight loss intervention on bone mineral density in type 2 diabetes: results from the look AHEAD randomized trial. *J. Bone Miner. Res.* **27,** 619–627
17. Chao, D., Espeland, M. A., Farmer, D., Register, T. C., Lenchik, L., Applegate, W. B., and Ettinger, W. H., Jr. (2000) Effect of voluntary weight loss on bone mineral density in older overweight women. *J. Am. Geriatr. Soc.* **48,** 753–759
18. Ronis, M. J., Chen, Y., Badeaux, J., and Badger, T. M. (2009) Dietary soy protein isolate attenuates metabolic syndrome in rats via effects on PPAR, LXR, and SREBP signaling. *J. Nutr.* **139,** 1431–1438
19. Bhathena, S. J., and Velasquez, M. T. (2002) Beneficial role of dietary phytoestrogens in obesity of diabetes. *Am. J. Clin. Nutr.* **76,** 1191–1201
20. Nagata, C., Shimizu, H., Takami, R., Hayashi, M., Takeda, N., and Yasuda, K. (2002) Soy product intake and serum isoflavonoid and estradiol concentrations in relation to bone mineral density in postmenopausal Japanese women. *Osteoporos. Int.* **13,** 200–204
21. Palacios, C. (2006) The role of nutrients in bone health, from A to Z. *Crit. Rev. Food Sci. Nutr.* **46,** 621–628
22. Kim, M. S., and Lee, Y. S. (2005) Effects of soy isoflavone and/or estrogen treatments on bone metabolism in ovariectomized rats. *J. Med. Food* **8,** 439–445
23. Cederroth, C. R., Vinciguerra, M., Gjinovci, A., Kuhne, F., Klein, M., Cederroth, M., Caille, D., Suter, M., Neuman, D., James, R. W., Doerge, D. R., Wallimann, T., Meda, P., Foti, M., Rohner-Jeanrenaud, F., Vassalli, J. D., and Nef, S. (2008) Dietary phytoestrogens activate AMP-activated protein kinase with improvement in lipid and glucose metabolism. *Diabetes* **57,** 1176–1185
24. Badger, T. M., Ronis, M. J. J., Wolff, G., Stanley, S., Ferguson, M., Shankar, K., and Jo, C.-H. (2008) Consumption of soy protein isolate reduces hepatosteatosis in obese yellow agouti (Avy) mice, but does not alter the coat color phenotype. *Exp. Biol. Med. (Maywood)* **233,** 1242–1254
25. Watkins, B. A., Reinwald, S., Li, Y., and Seifert, M. F. (2005) Protective actions of soy isoflavones and n-3 PUFAs on bone mass in ovariectomized rats. *J. Nutr. Biochem.* **16,** 479–488
26. Wu, J., Wang, X., Chiba, H., Higuchi, M., Nakatani, T., Ezaki, O., Cui, H., Yamada, K., and Ishimi, Y. (2004) Combined intervention of soy isoflavone and moderate exercise prevents body fat elevation and bone loss in ovariectomized mice. *Metabolism* **53,** 942–948
27. Cao, J. J., Gregoire, B. R., and Gao, H. (2009) High-fat diet decreases cancellous bone mass but has no effect on cortical bone mass in the tibia in mice. *Bone* **44,** 1097–1104
28. Chen, J. R., Lazarenko, O. P., Haley, R. L., Blackburn, M. L., Badger, T. M., and Ronis, M. J. (2009) Ethanol impairs estrogen receptor signaling resulting in accelerated activation of senescence pathways, whereas estradiol attenuates the effects of ethanol in osteoblasts. *J. Bone Miner. Res.* **24,** 221–230
29. Solinas, G., Naugler, W., Galimi, F., Lee, M. S., and Karin, M. (2006) Saturated fatty acids inhibit induction of insulin gene transcription by JNK-mediated phosphorylation of insulin-receptor substrates. *Proc. Natl. Acad. Sci. U. S. A.* **103,** 16454–16459
30. Chen, J. R., Singhal, R., Lazarenko, O. P., Liu, X., Hogue, W. R., Badger, T. M., and Ronis, M. J. (2008) Short term effects on bone quality associated with consumption of soy protein isolate and other dietary protein sources in rapidly growing female rats. *Exp. Biol. Med. (Maywood)* **233,** 1348–1358
31. Cimino, C. O., Shelnutt, S. R., Ronis, M. J., and Badger, T. M. (1999) An LC-MS method to determine concentrations of isoflavones and their sulfate and glucuronide conjugates in urine. *Clin. Chim. Acta* **287,** 69–82
32. Gu, L., Laly, M., Chang, H. C., Prior, R. L., Fang, N., Ronis, M. J., and Badger, T. M. (2005) Isoflavone conjugates are underestimated in tissues using enzymatic hydrolysis. *J. Agric. Food Chem.* **53,** 6858–6863
33. Zhang, J., Lazarenko, O. P., Wu, X., Tong, Y., Blackburn, M. L., Gomez-Acevedo, H., Shankar, K., Badger, T. M., Ronis, M. J., and Chen, J. R. (2012) Differential effects of short term feeding of a soy protein isolate diet and estrogen treatment on bone in the pre-pubertal rat. *PLoS One* **7,** e35736
34. Chen, J. R., Zhang, J., Lazarenko, O. P., Kang, P., Blackburn, M. L., Ronis, M. J., Badger, T. M., and Shankar, K. (2012) Inhibition of fetal bone development through epigenetic down-regulation of HoxA10 in obese rats fed high-fat diet. *FASEB J.* **26,** 1131–1141
35. Chan, M. E., Adler, B. J., Green, D. E., and Rubin, C. T. (2012) Bone structure and B-cell populations, crippled by obesity, are partially rescued by brief daily exposure to low-magnitude mechanical signals. *FASEB J.* **26,** 4855–4863
36. Nolan, C. J., Madiraju, M. S., Delghingaro-Augusto, V., Peyot, M. L., and Prentki, M. (2006) Fatty acid signaling in the beta-cell and insulin secretion. *Diabetes* **55**(Suppl. 2), S16–S23
37. Clemens, T. L., and Karsenty, G. (2011) The osteoblast: an insulin target cell controlling glucose homeostasis. *J. Bone Miner. Res.* **26,** 677–680
38. Holzer, R. G., Park, E. J., Li, N., Tran, H., Chen, M., Choi, C., Solinas, G., and Karin, M. (2011) Saturated fatty acids induce c-Src clustering within membrane subdomains, leading to JNK activation. *Cell* **147,** 173–184
39. Das, M., Jiang, F., Sluss, H. K., Zhang, C., Shokat, K. M., Flavell, R. A., and Davis, R. J. (2007) Suppression of p53-dependent senescence by the JNK signal transduction pathway. *Proc. Natl. Acad. Sci. U. S. A.* **104,** 15759–15764
40 Fuchs, S. Y., Adler, V., Pincus, M. R., and Ronai, Z. MEKK1/JNK signaling stabilizes and activates p53. (1998) *Proc. Natl. Acad. Sci. U. S. A.* **95,** 10541–10546
41. Spallarossa, P., Altieri, P., Barisione, C., Passalacqua, M., Aloi, C., Fugazza, G., Frassoni, F., Podestà, M., Canepa, M., Ghigliotti, G., and Brunelli, C. (2010) p38 MAPK and JNK antagonistically control senescence and cytoplasmic p16INK4A expression in doxorubicin-treated endothelial progenitor cells. *PLoS One* **5,** e15583
42. Elbaz, A., Wu, X., Rivas, D., Gimble, J. M., and Duque, G. (2010) Inhibition of fatty acid biosynthesis prevents adipocyte lipotoxicity on human osteoblasts in vitro. *J. Cell. Mol. Med.* **14,** 982–991
43. Fazeli, P. K., Horowitz, M. C., Macdougald, O. A., Scheller, E. L., Rodeheffer, M. S., Rosen, C. J., and Klibanski, A. (2013) Marrow fat and bone: new perspectives. *J. Clin. Endocrinol. Metab.* **98,** 935–945
44. Blake, C., Fabick, K. M., Setchell, K. D., Lund, T. D., and Lephart, E. D. (2011) Neuromodulation by soy diets or equol: anti-depressive & anti-obesity-like influences, age- & hormone-dependent effects. *BMC Neurosci.* **12,** 28
45. Chen, X., Garner, S. C., Quarles, L. D., and Anderson, J. J. (2003) Effects of genistein on expression of bone markers during MC3T3-E1 osteoblastic cell differentiation. *J. Nutr. Biochem.* **14,** 342–349
46. Torre-Villalvazo, I., Gonzalez, F., Aguilar-Salinas, C. A., Tovar, A. R., and Torres, N. (2009) Dietary soy protein reduces cardiac lipid accumulation and the ceramide concentration in high-fat diet-fed rats and ob/ob mice. *J. Nutr.* **139,** 2237–2243
47. Chen, J. R., Lazarenko, O. P., Blackburn, M. L., Badeaux, J. V., Badger, T. M., and Ronis, M. J. (2009) Infant formula promotes bone growth in neonatal piglets by enhancing osteoblastogenesis through bone morphogenic protein signaling. *J. Nutr.* **139,** 1839–1847
48. Villareal, D. T., Chode, S., Parimi, N., Sinacore, D. R., Hilton, T., Armamento-Villareal, R., Napoli, N., Qualls, C., and Shah, K. (2011) Weight loss, exercise, or both and physical function in obese older adults. *N. Engl. J. Med.* **364,** 1218–1229
49. Jensen, L. B., Quaade, F., and Sørensen, O. H. (1994) Bone loss accompanying voluntary weight loss in obese humans. *J. Bone Miner. Res.* **9,** 459–463

Received for publication January 3, 2013.
Accepted for publication May 14, 2013.